Chemical Engineering Science, Vol. 42, No. 7, pp. 1553–1564, 1987.
Printed in Great Britain.

0009–2509/87 $3.00 + 0.00

NETWORK MODEL FOR STRAINING DOMINATED PARTICLE ENTRAPMENT IN POROUS MEDIA

S. D. REGE and H. S. FOGLER
Department of Chemical Engineering, The University of Michigan, Ann Arbor, MI 48109, U.S.A.

(*Received* 27 *March* 1986; *accepted* 26 *September* 1986)

Abstract—A network model has been developed to study and describe formation damage resulting from particle entrapment in porous media by straining or size exclusion. Unlike the previous network models, this model considers the simultaneous entry of a number of particles into the network, as well as the effects of fluid flow on the particle transport path. A systematic study has been carried out on the flow and entrapment of monodispersed particles as well as particles with a size distribution through different networks. The effects of various parameters such as network size, particle size distribution and pore size distribution on the extent of formation damage, manifested by permeability reduction have been discussed in this paper. The model has also been used to determine the degree of prefiltration required to prevent damage to injection wells during water flooding. The model predictions show good agreement with experimental data for several different runs. A single parameter is used to match the exact number of pore volumes required to produce damage to the porous media. This parameter was found to be constant for the two different sandstones studied and for different concentrations of particles in the suspension. The simulation was also performed using the "random walk model" (which does not account for the fluid flow effects on particle flow) for purposes of comparison. The permeability responses predicted by this random walk model show trends that are significantly different from those observed experimentally. The network model developed in this paper has wide application in water flooding and matrix acidizing operations where diverting agents are used.

INTRODUCTION

Many engineering processes involve the transport and capture of particles in disordered media. One application is found in enhanced oil recovery which often involves a series of processes such as water flooding, preflushing and acidization. During these operations, it is necessary to take precautions to prevent formation damage caused by particles in the injected fluid. In many water flooding operations the major problem lies in the inadequate maintenance of the well. The water that is injected usually contains particulate matter of various sizes. These particulates may plug the pores thereby reducing the permeability and damaging the formation. Consequently it is usually necessary to filter the water prior to injection. Filtration of large volumes of water, as used during water flooding operations, is expensive. To minimize this cost, unnecessary filtering of the very fine particles needs to be avoided. Thus the question often asked in such applications is—what is the minimum amount of prefiltration of the injection water that is necessary to prevent extensive damage to the formation? This is one of the key questions that this study has addressed.

Another operation requiring an effect almost opposite to the one above is the use of diverting agents to obtain uniform matrix acidization. The porous medium is generally heterogenous and contains dominant flow paths. These paths become preferentially acidized as they carry more acid than other channels and this results in preferential stimulation. Diverting agents serve to partially block the dominant channels and thereby increase the acid flow through other parts of the formation. In these operations it is necessary to accurately determine the concentration and size distribution of the diverting agents prior to the injection. An error in the estimation of these factors can cause extensive damage to the formation rather than uniform stimulation.

To achieve an understanding of the particulate processes in the porous media, a model based on the concept of a "damage wave front", progressing through a triangular network of tubes has been developed. In this model a number of particles enter the formation simultaneously and their path through the network is governed by another concept, i.e. flow biased probability.

The present work considers straining or size exclusion to be the dominant mechanism of capture of the particles in the porous media. Work on deep bed filtration (Herzig *et al.*, 1970; Tien and Payatakes, 1979) has shown that other capture mechanisms also exist, and due to these mechanisms entrapment of particles smaller than the pore throats can also occur. While deep bed filtration theories, especially those based on the trajectory analysis (Tien and Payatakes, 1979), have successfully predicted the filter coefficients and filter efficiency (in some cases) they have however not been effective in providing a good estimate of the changes in the pressure drop encountered during the filtration process. It is also evident that when large size particles are present and straining occurs, the resulting damage is more severe than that caused by the gradual deposition of the smaller particles. The effects of dominant parameters such as particle size distribution and pore size distribution on the extent of formation damage will be discussed. The concepts of percolation

theory have been applied to show that a representative prediction of the formation damage can be obtained only if sufficiently large networks are used. The model predictions have been compared with experimental observations for different sandstone cores and different concentrations of particles in the effluent suspension. The agreement was found to be good for these cases. Model predictions based on a 'random walk model", however, did not agree with experimental data indicating that fluid flow effects on particle flow and the concept of damage wave front are important factors for realistic predictions.

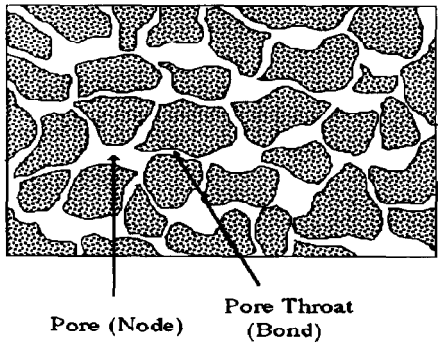

Fig. 1. Schematic representation of the porous media showing pore throats and pore chambers.

MODEL FORMULATION

1. *Model representation of the porous media*

To study particulate processes in porous media it is necessary to select a model to represent the porous media. Photomicrographs of a porous media (Dullien and Dhawan, 1974; Yadav *et al.*, 1984) show that one of the basic properties of the media is interconnections, as is shown schematically in Fig. 1. Recent studies using pore castings with woods metal (Wardlaw, 1976) and 3-D SEM photographs (Porter, 1985) give further evidence that the porous media consists of large pore spaces which are connected by narrow constrictions. These constrictions, which have different size distributions depending on the type of media, offer the major resistance to the fluid flow. The network model originally presented by Fatt (1956) was selected to represent the porous matrix as it satisfies the major structural property (i.e. interconnections) of the porous media. Cylindrical bonds in the network represent the constrictions, and the nodes represent the pore chambers (Fig. 2). It has been shown by Fatt that certain static and dynamic properties of the porous media predicted by the network model are similar to those observed experimentally. Recent work on network modelling (Jerauld *et al.*, 1984) has shown that a regular triangular network has the same coordination number as a random Voronoi lattice. Besides being a very realistic representation of the porous media, the regular triple hexagonal lattice has the added advantage of allowing the numerical calculations to be performed more efficiently. For these reasons the regular triangular network has been selected to represent the porous media. The network models have previously been used to study various processes such as fluid displacements in porous media (Simon and Kelsey, 1971), dispersion in disordered media (Sahimi *et al.*, 1983) and others (Yortsos and Sharma, 1986; Siegel and Langer, 1986; Lapidus *et al.*, 1985).

Adopting the network model for studying particle plugging also offers two major advantages:

(a) simultaneous accounting of particles that are migrating and those that are trapped can be made, and
(b) direct monitoring of the change in permeability due to the filtration process is possible, i.e. no empirical correlation is required to relate the amount of material deposited to the change in permeability.

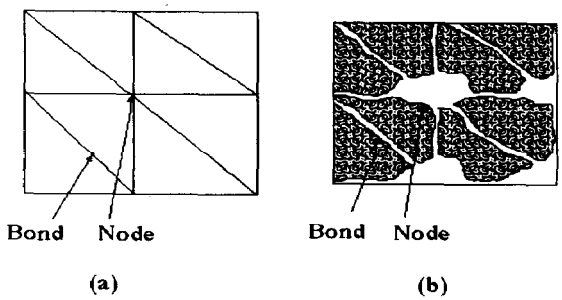

Fig. 2. Network representation of the porous media. Schematics show similarity between the network model and the porous media.

2. *Network construction*

The porous media is heterogenous in nature and large differences in the static, dynamic and structural properties may exist for different porous formations. These heterogenities can be attributed to the difference in the pore size distributions in the formation. To represent the porous media realistically the bond size distribution of the network should be similar to the pore throat size distribution existing in the formation being considered. The actual pore throat size distribution is determined from mercury porosimetry and photomicrography (Dullien and Dhawan, 1974) performed on a sample of the formation. A similar distribution is then assigned randomly to the radius of the bonds throughout the network. Different studies (Fatt, 1956; Rose, 1957) have assigned lengths to the bonds by various methods: constant length, length directly proportional or inversely proportional to the radius, and lengths having a size distribution with a mean and standard deviation similar to that of the radii (i.e. no specific relationship exists between the length and radius of an individual bond). While network model predictions for porous media properties based on all these methods agree well with experimental observations the last method was selected for the following reasons:

(1) the porous media is considered to be isotropic and the distribution of the pore lengths can be considered to be the same as the pore radius distribution, and
(2) the other relationships require the use of a proportionality constant which is an adjustable parameter. This introduces a degree of uncertainity in the model predictions.

3. *Calculation of fluid flow*

Having generated the network, the next step of the simulation involves the calculation of the fluid flow through each of the bonds. In order to do this, the fluid pressure at each node is calculated, and the flow rate in each tube is determined from the Hagen Poiseuille equation. To determine the nodal pressures, mass balance equations are written around every node using the standard periodic wrap around boundary condition. The wrap around boundary condition allows particles at the bottom of the network to flow to corresponding nodes at the top. This in effect eliminates the structural anistropy which would otherwise cause more particles to flow to the bottom of the network (see Fig. 2). For an M by N network, there are $M \times N$ unknowns (the pressure at the $M \times N$ nodes) and therefore $M \times N$ equations. These equations form a sparse matrix (banded in this case) and can be solved using Gaussian Elimination for the injection conditions of either constant pressure or constant flow rate. It will be shown later that relatively large networks are required to predict results representative of the system, and in these cases the number of equations to be solved are fairly large (about 2500 equations). To solve these equations efficiently, the supercomputer Cray X-MP was used. It is important to note that since all the mass balance equations are solved simultaneously, the flow through each bond is dependent not only on the size of that particular bond but also on the resistance offered to flow by connecting bonds upstream and further downstream in the network. The banded nature of the equations also makes it possible to consider relatively large size networks, since the elimination process is more efficient.

4. *Flow of particles*

In the present model the particles move through the bonds with the average velocity of the fluid in that bond. It has been shown by Leichtberg *et al.* (1976) that even for large ratios of particle diameter to bond diameter (as high as 0.95) the deviation of particle velocity from the average fluid velocity is negligible. For this reason momentary perturbations in fluid velocities due to particles have been neglected. The previous network model (Todd *et al.*, 1984) used for studying the migration of injected fines has predicted results which are not in qualitative or quantitive agreement with experimental results. In their model, Todd and coworkers consider only one particle at a time and its path is traced randomly through the network until it is captured. This approach of considering only one particle at a time is unrealistic, especially in the case of suspensions with a high concentration of particles where a number of particles enter the formation simultaneously. Another reason for the discrepancy in their model predictions and experimental results is that no consideration is given to the influence of fluid flow on the path chosen by a particle when it reaches any node. A "random walk" approach was used, whereby, a particle at a node chooses its exit path randomly. While this does indeed take into account the "stochastic" nature of the filtration process, it neglects the flow rate effect. In Fig. 3, for example, if a suspension of many tracer particles (all smaller in size than tube C) is injected into tube A, 99% of the total particles would pass through tube B. However the random walk model predicts that only 50% of the total particles would pass through tube B, and therefore a major modification of the random walk model is warranted.

The proposed model uses the concept of flow biased probabilities (as opposed to the "random" walk) to trace the particle path through the network. Also a new concept termed the wave-front movement has been developed to pass a number of particles simultaneously through the network. These concepts are described below in detail.

(a) *Flow-biased probability.* The filtration process in the porous media is stochastic in nature, in that an experiment repeated under similar conditions could exhibit scatter in the permeability or pressure drop responses. To take this stochastic nature into account, the previous network model by Todd *et al.* (1984) considered the particles undergoing a random walk within the network. However, simple RTD experiments (as in Fig. 3) show that given a choice of paths a particle has a greater probability of following a path with a greater flow rate. Thus, to make the model realistic, one needs to incorporate the effects of "probability" and "flow rate". These effects have been combined into the concept of "flow-biased probability".

In the present model when a particle encounters a node in the network, it has a choice of exit paths. The exit channel is selected randomly, but with a bias toward the paths with greater flow rates. Based on the flow rate through each path, a probability is assigned to that path. The greater the flow rate, the greater the probability of the particle choosing that path. In Fig. 4

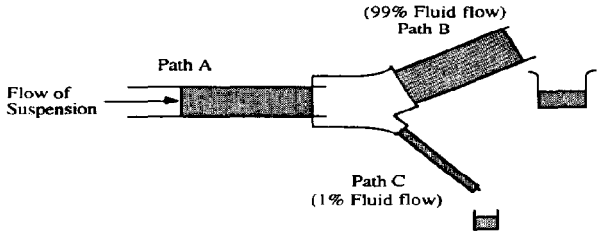

Fig. 3. Schematic to describe the differences in the random walk assumption and flow-biased probability.

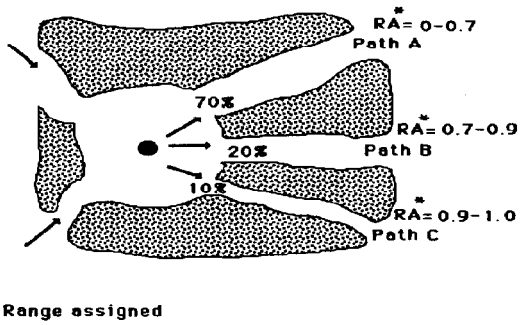

Fig. 4. Schematic representation of the flow-biased probability for particle flow in porous media.

for example, the particle has a greater probability of choosing path A, as compared to path B or C. During the simulation, a certain range is assigned to each path. The size of this range, RA, corresponds to the fraction of the exiting flow passing through that particular bond. A random number is then generated and the range within which this number falls determines the path chosen by the particle. In Fig. 4, if the random number generated is 0.5, then path A is chosen. However, if the random number is 0.95 then path C is selected even though it has the lowest flowrate. Since a larger flow fraction implies a greater possibility of the random number lying within the corresponding range, the "flow rate" effect is taken into account. The random generation process involved in making the choice of path preserves the stochastic nature of the actual filtration process.

(b) "*Wave-front*" *movement*. The "wavefront" movement essentially consists of using small discrete time steps during which the particles move various distances through the network. A pseudo-steady state assumption is made that the events occurring during this time step are simultaneous. Several particles (the actual number depending on the time step, concentration, and flow rate) are selected from a specified particle size distribution. The probability of selecting a particle of a certain radius is proportional to the density function of the particle size distribution. These particles are then placed randomly at the nodes on the entry face. The actual number of particles at each entry node is proportional to the flow rate entering that node. The inherent assumption made here is that the local concentration of particles in the suspension is uniform. The particles (at the entrance and within the network) then advance forward during each time step. When a particle encounters a node, the choice of path is made by means of "flow-biased" probability described above. During a given time step different particles travel different distances through the network depending on whether a slow or a fast path is selected. If during its journey, a particle encounters a pore whose size is smaller than that of the particle, it gets captured and the bond is plugged. This is the size exclusion or straining mechanism of capture. Particles smaller than the bonds, however, are allowed to pass through. Any particle arriving at a bond after it has been plugged (but during the same time step) is also assumed to be captured. After all the particles in the network have been advanced forward by one time step, the flow through the network is redistributed to account for the blocked pores and the overall change (increase) in the pressure drop is recalculated. As a result, the flow biased probability for the bonds also changes throughout the network. The permeability ratio (for a constant flow rate system) is then calculated as the ratio of the initial pressure drop to the pressure drop at any time. The results are reported as the permeability change of the formation as a function of the number of pore volumes injected, where a single pore volume is defined as the fluid volume present in the bonds in the network.

RESULTS AND DISCUSSION

The network model for plugging is stochastic in nature due to the degree of randomness involved in laying down the network, selecting particle path at a node and generating different size particles at the entry face. Due to this, several computer runs need to be performed under identical physical conditions, but with different initial seeds for the random number generator so that different networks are generated. These different networks with essentially the same pore size distribution are called realizations.

Monodispersed particles

In the limiting case of passing monodispersed particles through a network with a distribution of bonds the scatter in predictions, as expected, was found to be very small for any particular realization. The ratio of the permeability at any time, t, to the initial permeability, $K/K0$, is shown as a function of the number of pore volumes injected (in arbitrary units) in Fig. 5. For the baseline case illustrated in Fig. 5, the monodispersed particles have a size of one unit ($D_{pa} = 1$) and the bonds are assigned a normal size distribution with a mean size of one unit ($D_{pu} = 1$) and a standard deviation of 0.33 units ($\sigma_{po} = 0.33$). The

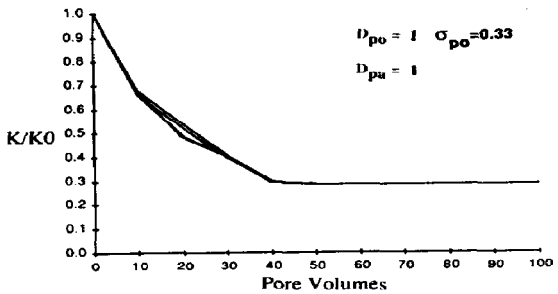

Fig. 5. Model predictions for a 10 × 50 network with different initial random number seeds. The curves lie close to each other indicating small scatter.

simulation is however not restricted to a normal distribution and other forms of distribution such as log–normal or uniform distributions can also be used. The particle concentration in the suspension for the baseline case is 1×10^8 particles per unit volume. One observes from Fig. 5 that for monodispersed particles it is reasonable to consider just one run to be a representative prediction. Furthermore after a sufficiently long time, the permeability ratio attains a constant value, implying that most of the pores with diameters smaller than the particle size have been plugged up.

To determine whether the above predictions are truly representative, the simulation for particle plugging was performed with different network sizes having the same width (10 nodes in this case). One observes from Fig. 6 that the scatter was not only large, but in one instance, for the 10×80 network, total plugging occurred after only a few pore volumes were injected.

However, when different realizations were carried out for the 10×80 network (Fig. 7) only partial plugging occurred in some runs. The reason for such a large discrepancy in predictions arises due to the relatively small size of the network used. These effects of network size on the prediction of the plugging phenomenon can be elucidated by percolation theory. In percolation theory a certain fraction of the bonds in the network, p, are laid down and then the probability of percolation is determined. Analogously in filtration, after a sufficiently long time a certain fraction of the bonds, $1-p$, are plugged. Whether the plugging of these bonds leads to total or partial plugging is related to the probability of percolation. For the examples considered in Figs 4–6 the particle size, D_{pa}, is one unit which corresponds to the mean bond size, D_{po}. Since the bond size distribution follows a normal distribution density function half the bonds in network would have a size smaller than D_{pa}. All these bonds with a size smaller than D_{pa} would get plugged if a sufficiently large number of pore volumes of suspension are injected into the network. The final fraction p of unplugged bonds would then be 0.5, and from the percolation probability curves (Fig. 8) the probability of percolation for a 10×80 network is about 0.96. This implies that for the 10×80 network there are some realizations (the probability of their occurrence is about 4%) for which total plugging would be predicted and others where only partial plugging would occur. It is necessary to eliminate such large degrees of scatter in model predictions to obtain realistic results. For relatively large networks the percolation probability curves become steeper (Fig. 9) and for very large networks we can essentially eliminate the possibility of getting unreliable predictions of low probability as in the case of the 10×80 network.

Scaling theories (Fisher, 1971) have been developed to determine a representative network size in percolation problems. In our case however, the bonds in the network have a size distribution and the model predictions are time dependent. Consequently, while

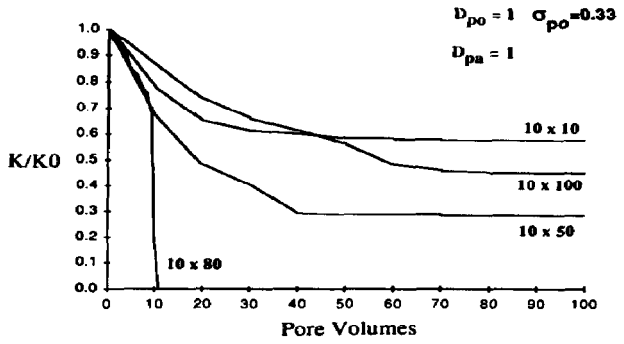

Fig. 6. Model predictions for networks with relatively small sizes. Different size networks predict results exhibiting large scatter.

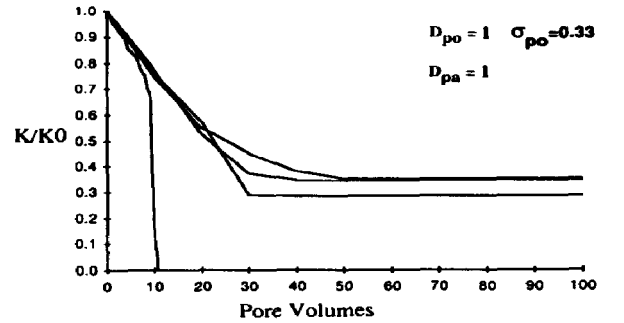

Fig. 7. Different realizations for the 10×80 network show that total plugging occurs only in some cases.

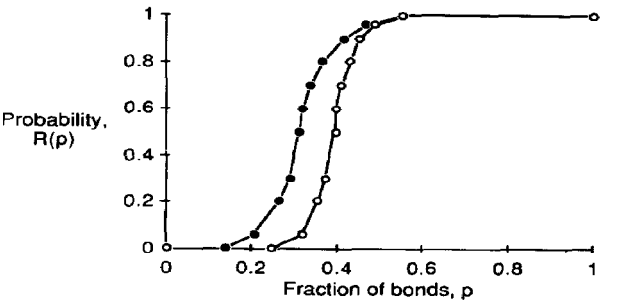

Fig. 8. Percolation probability curves for relatively small size networks show a gradual increase in the slope. Legend: —●— 10×10 network, —O— 10×100 network.

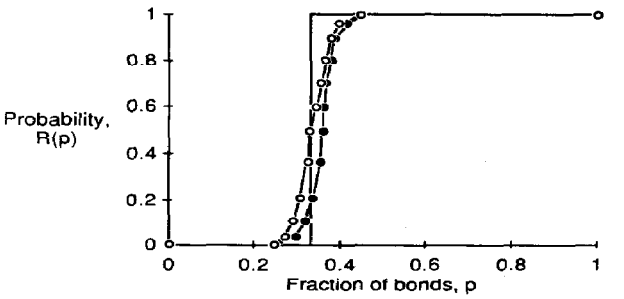

Fig. 9. Percolation probability curves for relatively large size networks exhibit sharp increases in the slope. Legend: —O— 20×20 network, —●— 20×100 network, —— very large network.

the network size determined from scaling theory may not be truly representative for the particle entrapment phenomenon it is a good first estimate. The representative size of networks used in the simulations discussed here is 40 × 40 which is a first estimate obtained from scaling theory. For a 40 × 40 network we see that the curves in Fig. 10 lie fairly close to each other and the range of scatter is small. While large networks give realistic predictions, the storage space and time required to run the simulation in these cases is extremely high. The advent of the supercomputer Cray, however, has made these simulations feasible. To increase the efficiency of solving the mass balance equations and to reduce the time for each run, the use of the supercomputer Cray X-MP was necessary. Even when working with representative size networks, several runs and realizations need to be performed to reduce the degree of scatter, especially for broad pore and particle size distributions.

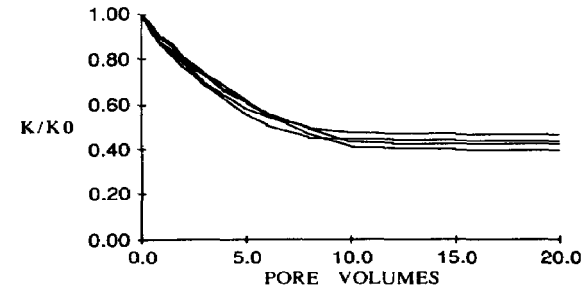

Fig. 10. Different realizations for relatively large (40 × 40) networks show small scatter.

Polydispersed particles

The results discussed so far have been for monodispersed particles. In reality however, the particles injected would have a size distribution and the model predictions for these cases are reported below. The effects of two factors on the extent of formation damage are discussed here: the mean particle size and the standard deviation.

In the present study, a truncated normal distribution is assigned randomly to the bonds in the network and to the particles in the suspension. For the baseline case the bonds are assigned a mean size of one unit (D_{po} = 1) and a standard deviation of 0.5 units (σ_{po} = 0.5). The effects of mean size and standard deviation, have been studied by varying the mean size and the standard deviation of the particles. Since the simulation is stochastic in nature an average curve is obtained by performing Monte Carlo simulations on four realizations and 15 runs with each realization.

Effect of mean size of particles and pores

The effects of mean size for three sample cases can be explained qualitatively by means of Fig. 11. In Fig. 11A the mean sizes of the pore size distribution and the particle size distribution are relatively far apart and therefore the extent of overlap is low. In Fig. 11C, the distributions are virtually similar and therefore the extent of overlap is high. The model predictions for these three cases are shown in Fig. 12 in terms of the permeability ratio ($K/K0$) as a function of the number of pore volumes injected. We see that the model predicts a relatively gradual decline in the permeability ratio for case A, while for case C this decline occurs 10 times faster. As expected intuitively, the number of pore volumes required for a drastic reduction in the permeability ratio decreases as the extent of overlap between the pore and particle size distributions increases. Model predictions for several other cases of mean size and standard deviation will be discussed in later sections.

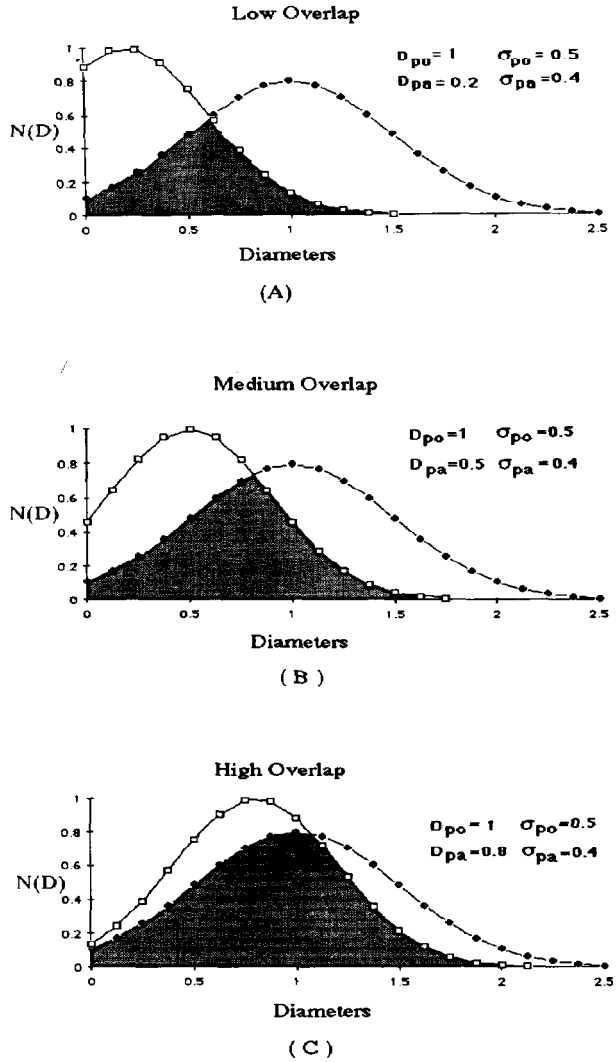

Fig. 11. Effects of mean size on formation damage.

Effect of standard deviation of particle and pore sizes

For a given mean particle and pore size, the extent of damage is dependent on the standard deviations of the

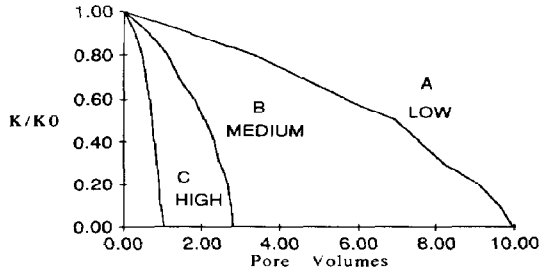

Fig. 12. Model predictions showing mean size effects for the three cases considered in Fig. 11.

particle and pore size distributions. In the case of varying standard deviation, it was found that both the extent and region of overlap affect the permeability decline. Three different cases for variations in the standard deviation are shown in Fig. 13. Figure 13B and C both have the same extent of overlap and this overlap is greater than that for Fig. 13A. Also the region of overlap is different in Fig. 13B and C since in case B, the pores have a broader distribution and in case C, the particles have a broader distribution. In Fig. 13C, for example, it is possible for a larger particle to plug up the relatively larger pores and cause greater damage (greater reduction in permeability) than in case B. The model predictions for three corresponding cases are shown in Fig. 14. The curves show that for case A the decline in permeability was relatively slow, but as expected damage occurred faster for case C than for case B. Several other cases have been considered and the combined effect of mean size and standard deviation are shown in Figs 15 and 16 in terms of the number of pore volumes required to reduce the network permeability to 1% of its initial value as a function of the ratio of the pore and particle standard deviations (σ_{po}/σ_{pa}). Each curve in Figs 15 and 16 represents a constant value of the mean size ratios. The dotted lines in the Figs 15 and 16 represent the linear regression fit for this region, and the correlation coefficient was greater than 0.97 in all cases. Model predictions for the number of pore volumes required to reduce the permeability ratio below 1% are similar to those shown in Figs 15 and 16, mainly because damage beyond 1% takes place very rapidly. The simulation was also performed for higher values of σ_{po}/σ_{pa}. In these cases the number of pore volumes required to cause a permeability reduction of 1% (by straining) was found to be extremely high. This essentially implies that at high values of σ_{po}/σ_{pa} the permeability decline due to straining will not be significant and deep bed filtration effects will start dominating. The region of interest for straining conditions is therefore in the lower values of the abscissa.

Comparison of model predictions with experimental data

There is very limited filtration data in the literature for straining dominated capture in porous media. For

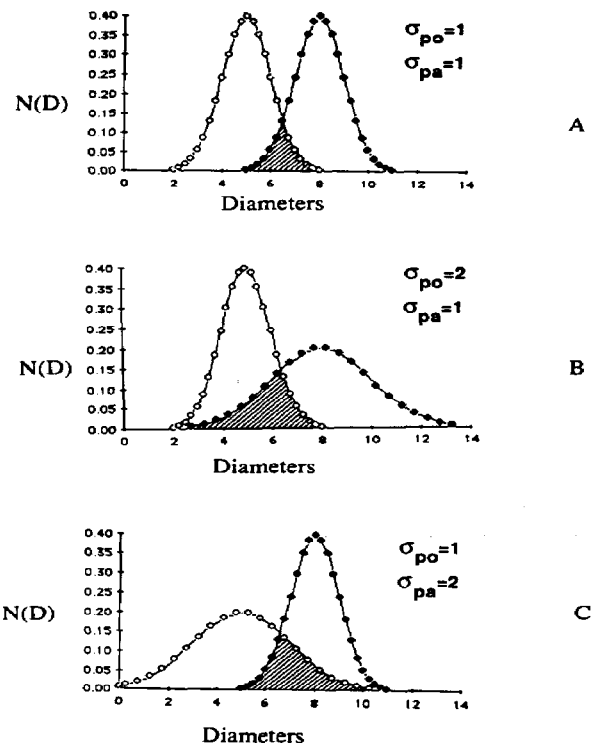

Fig. 13. Effects of standard deviation on formation damage.

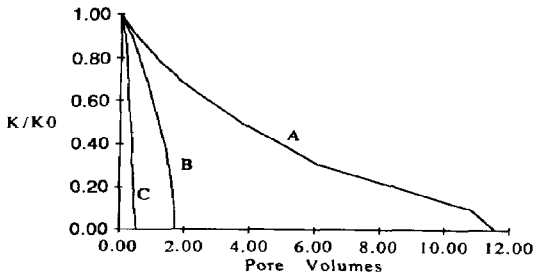

Fig. 14. Model predictions showing standard deviation effects for three cases similar to those described in Fig. 13.

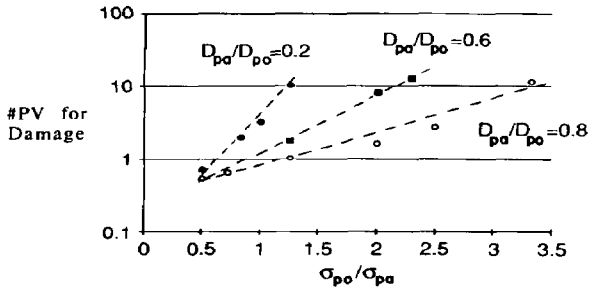

Fig. 15. Linearized plot showing size distribution effects on formation damage.

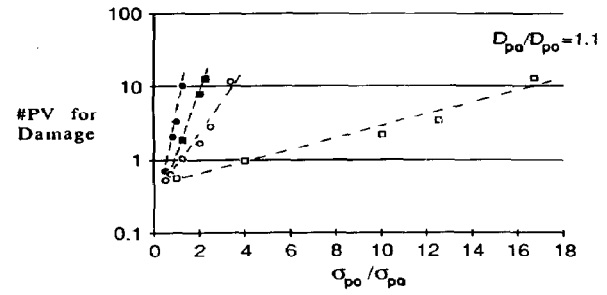

Fig. 16. Linearized plot showing size distribution effects over a wider range of mean size and standard deviation values.

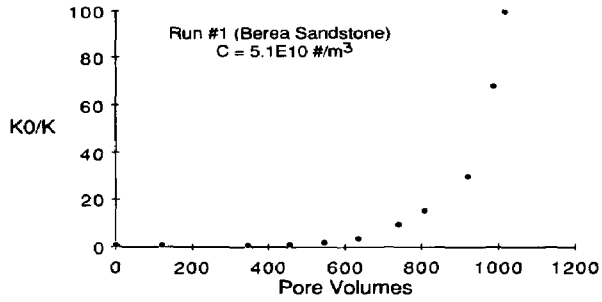

Fig. 17. A plot of inverse permeability ratio (i.e. $\Delta P/\Delta P_0$) vs pore volumes injected, obtained from core flood experiments by Donaldson and coworkers. Legend: ● data.

purposes of testing the model, the experiments of Donaldson *et al.* (1977) were used. Donaldson measured the pore size distribution (for different types of sandstones) and found that it followed a log–normal distribution. The particles they injected into the sandstone cores had similar distributions but different values for the geometric mean and the standard deviation. Some of the values reported in Donaldson's paper are tabulated in Table 1. The cores used for the experiments were 1.8 cm in diameter and 2.7 cm in length, and the flow rate used was 2.78 ml/min.

A typical experimental observation is shown in Fig. 17 where the inverse of the permeability ratio (the experimentally measured pressure drop ratio) is given as a function of the number of pore volumes injected. It can be seen from this figure that the increase in the pressure drop across the core as the suspended particles are injected is gradual at low pore volumes. This is due to the fact that initially a large number of flow paths are available, and plugging of some of these paths does not greatly affect the pressure drop. However as the major flow paths get plugged, the resistance to flow increases resulting in an increase in the pressure drop. Eventually the injected fluid suspension can flow only through the small pores and when these get plugged, the pressure drop increases catastrophically. These sharp increases in the pressure drop are typical of straining dominated particle entrapment and are in sharp contrast with the gradual increases observed during deep bed filtration.

The simulation was performed for the four different cases corresponding to Donaldson's experimental runs shown in Table 1. The network size used was 40 × 60 as determined earlier from percolation scaling theories. Since the network represents only a small cross section of the actual core, the flow rate used in the simulation is such that the fluid velocites in experiments and the model are identical. A comparison of the permeability response curves obtained from the model and experiments for Run 1 is shown in Fig. 18. The bold line represents the average curve for 15 runs and four realizations. The model predicts an initial gradual increase in the inverse permeability ratio and then catastrophic damage. We observe that this is in excellent qualitative agreement with the experimental data. It should be emphasized that the physical conditions (such as pore size distributions, particle size distributions, particle concentrations and flow rates) under which the simulation was performed were identical to the experimental conditions used by Donaldson. Furthermore this qualitative agreement between theory and experiments was obtained without the use of any adjustable parameter.

To obtain quantitative agreement, i.e. the number of pore volumes required to cause a certain decrease in the permeability ratio, only a single parameter is necessary. For Run 1 the parameter was found to have a value of 1.5. This parameter value indicates that the number of network pore volumes required for a certain damage to occur was 1.5 times smaller than in the actual core. A possible reason for this discrepancy between the model and experimental data arises due to the nature of the plugging process during straining dominated conditions and is further explained below.

An examination of Donaldson's (1977) core at the end of a run showed that the major damage occurred near the inlet face. This phenomenon was also observed in the network at the end of the simulation.

Table 1. Experimental conditions used by Donaldson *et al.* (1977) to study plugging in porous media

Run No.	Type of sandstone	Pore size distribution		Particle size distribution		Particle concn. [No./m^3 ($\times 10^{-10}$)]
		Mean, D_{po} (μm)	Std. dev., σ_{po} (μm)	Mean, D_{pa} (μm)	Std. dev., σ_{pa} (μm)	
1	Berea	0.178	4.78	4.0	1.46	5.1
2	Berea	0.178	4.78	4.0	1.46	10.4
3	Cleveland	0.175	4.29	6.7	1.86	4.5
4	Cleveland	0.175	4.29	6.7	1.86	9.5

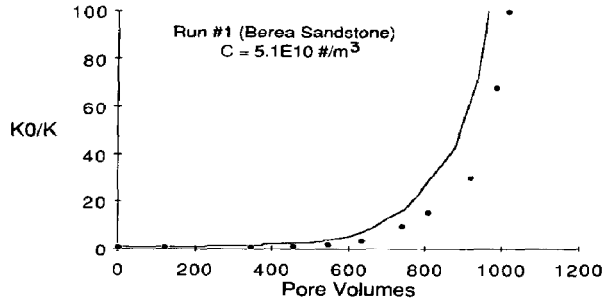

Fig. 18. A comparison of our model predictions with Donaldson's experimental data for Run 1. Legend: ● data, —— predictions.

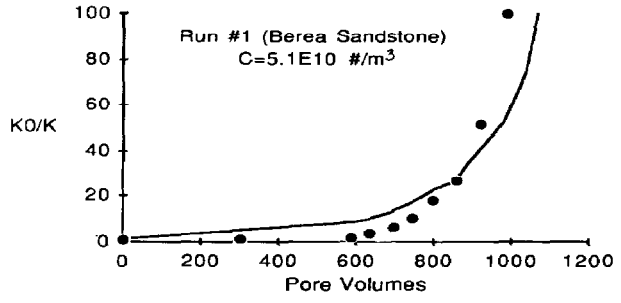

Fig. 19. Comparison of our model predictions obtained from a relatively small network with experimental data for Run 1. Legend: ● data, —— predictions.

Although plugging of the pore throats near the entry face is the primary cause for the permeability reduction, it is the volume of the pores in the *undamaged* and damaged zones which determines the actual *number* of pore volumes required to cause that permeability reduction. A fixed volume throughput of suspension which is responsible for damage would represent a relatively smaller *number* of pore volumes if the actual core was extremely long.

To determine the validity of the above reasoning we performed the simulation for a smaller network (40 × 40). In this case the actual volume of the bonds in the network is about 1.5 times smaller than in the network used in Fig. 18. Model predictions for this case were found to be in very good quantitative agreement with the experimental data without the use of any parameter (Fig. 19) thus supporting the proposed hypotheses. It should be noted however, that changes in the experimental core length would give a different value of the matching parameter.

Comparison of model predictions with experimental Runs 2–4 (Figs 20–22) led to an important conclusion. The value of the single pore volume parameter was found to be the same, i.e. 1.5, for all the different runs. Very good agreement was observed for Runs 1, 2, and 4 while the experimental curve for Run 3 showed some deviation from the model predictions. One possible explanation is that the filtration process is stochastic, and experimental runs carried out under identical conditions can exhibit scatter similar to that observed in the network model. The fact that this parameter value is invariant for different sandstones, different concentrations of injected particles and different pore and particle size distributions is very encouraging. It implies that only one experimental run needs to be performed to determine the value of the parameter to match pore volumes required for damage. Once this value has been obtained, damage for other cases can then be predicted.

For purposes of comparison, a random walk model similar to Todd *et al.*'s (1984) model was developed. The curves shown in Fig. 23 for Run 1 exhibit the difference in the shape of the curves obtained from the two models. The experimental data plotted on Fig. 23

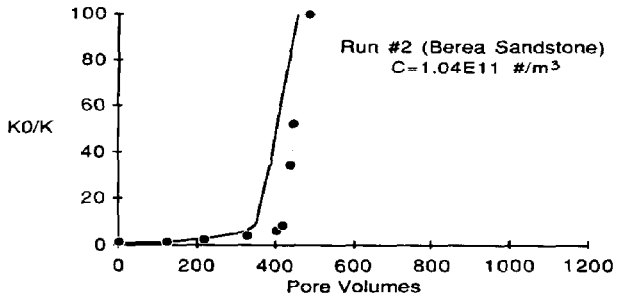

Fig. 20. Comparison of model predictions and experimental data for Run 2. Legend: ● data, —— predictions.

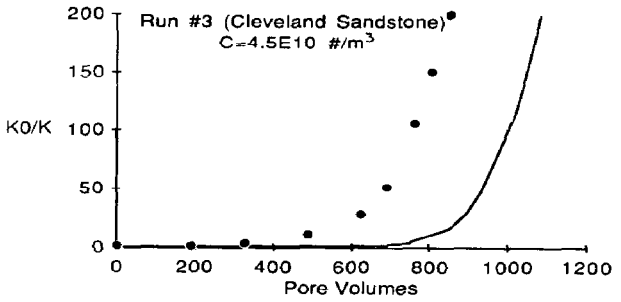

Fig. 21. Comparison of model predictions and experimental data for Run 3. Legend: ● data, —— predictions.

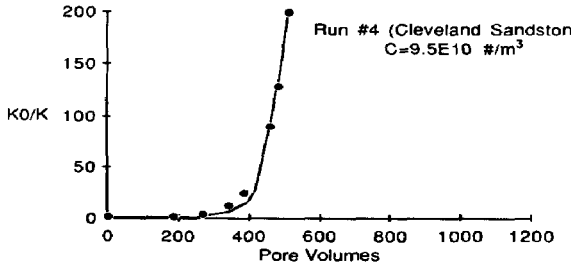

Fig. 22. Comparison of model predictions and experimental data for Run 4. Legend: ● data, —— predictions.

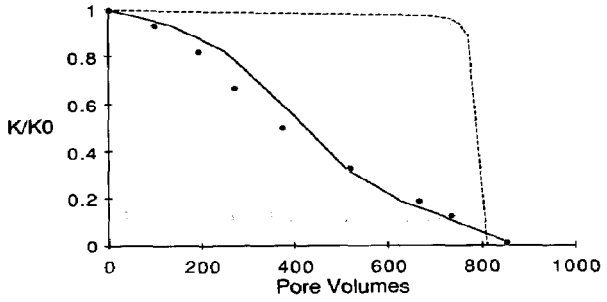

Fig. 23. Comparison of predictions by our model and the random walk model with experimental data. The model predictions obtained from our model have been scaled by 1.5 to obtain quantitative agreement with experimental data. Legend: ● data, —— flow biased probability, — — — random walk.

are the inverses of the measured pressure drop ratio. It can be observed that the predictions obtained from our model are in very good agreement with the experimental data, which is not the case for the random walk model. The random walk model predicts a very gradual initial decrease in the permeability ratio indicating that the major flow paths are not necessarily damaged during the early stages of the plugging process. However as the plugging continues only a few flow paths remain open (in general the paths with high flow rates), and when these get plugged the permeability ratio declines rapidly. Our model predicts that it is the major flow paths which get damaged initially as can be seen by the sharp monotonic decrease in the permeability ratio even in the early stages of the filtration process in Fig. 23. This trend was also observed in experiments performed by Donaldson *et al.* (1977).

The model developed in this paper to simulate the plugging phenomenon is essentially two-dimensional network with a coordination number of 6. It is encouraging that this 2-D model accurately simulated experimental runs performed on cylindrical 3-D cores. Changing the coordination number (in either a 2-D or 3-D network) would change the number of paths available for the flow of particles thereby affecting the volume throughput required to cause a certain amount of permeability reduction. However the volume of the network would also change by a corresponding amount. The final results plotted as $K/K0$ as a function of the number of pore volumes injected into the network would therefore be expected to remain unchanged.

A final point to be noted is that one might at first attribute the large increases in the pressure drop observed during Donaldson's experiments to the formation of a filter cake on the entry face. However, filter cake calculations (see Appendix) show that the maximum pressure drop due to filter cake resistance can be only 2 psig, while in experiments pressure drops as high as 400–700 psig were observed. This indicates that the major pressure drop was due to the plugging of the pores near the entry face and after this had occurred (responsible for major damage) the filter cake started to build up.

Effect of prefiltration of the injected fluid

As shown above, the model can accurately predict the extent of damage to the porous media due to the plugging of pores by particles suspended in the entering fluid. In water flooding operations it is necessary to prevent this damage by prefiltering the solids in the injected fluid. On one hand it is expensive to purchase and operate filters to remove the smaller particles, especially in the light of the large amounts of water used during water flooding. On the other hand, if only the larger particles are filtered out the injected fluid suspension may still damage the well. The effect of filtration is discussed by referring to Fig. 24. Filtering of the larger particles truncates the tail of the distribution and prevents plugging of the larger pores which carry most of the fluid. Three different cases of filter cut-off size are shown in Fig. 24. The filter cut-off size is the maximum particle size that is filtered prior to injection of the fluid into the formation. The actual value of the cut-off size is strongly dependent on the overlap between the particle and pore size distributions, which in turn depends on the mean sizes and standard deviations of the distributions.

The model predictions for three different cases of filter cut-off size are shown in Fig. 25. It is evident from this figure that decreasing the filter cut-off size reduces the extent of formation damage, e.g. one observes from Fig. 25 that if only particles greater than 1.2 units are filtered out, the resulting decline in permeability is still significant. If particles larger than the mean pore size

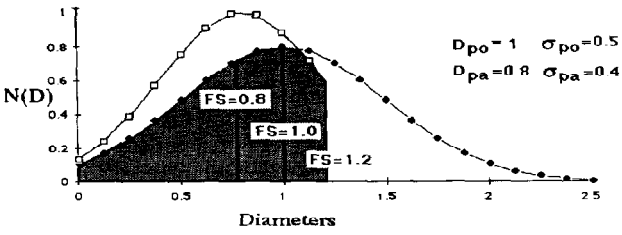

Fig. 24. Effects of pre-filtration on formation damage. Different cases of filter cut-off size are shown.

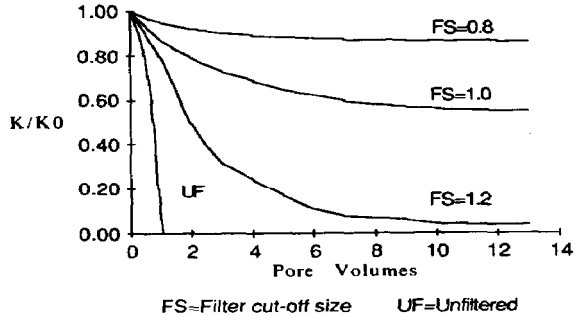

Fig. 25. Model predictions showing effects of pre-filtration on formation damage.

($FS = 1.0$) for example, are filtered out then the formation permeability would reduce to about 60% of its original value over a large period of time.

The model can thus predict the minimum cut-off point for prefiltration given the maximum damage permissible. It should however be noted that further reduction in permeability may be observed in reality due to deep bed filtration capture mechanisms, and the model predictions can be considered to be a first estimate for the filter cut-off size.

CONCLUSIONS AND SIGNIFICANCE

A different approach to modeling particle capture by the straining mechanism has been developed. This network model uses the wave front movement combined with flow-biased probability to predict the regimes of formation damage under straining dominant conditions. The model predicts that the damage which occurs due to straining is catastrophic and not gradual as in the case of classic deep bed filtration. An examination of the network at the end of run also indicated that this damage essentially occurred near the entry face of the core. Both these effects are in excellent agreement with experiments. A single parameter is used to quantitatively match the permeability response data. Runs carried out with two different types of sandstones and different concentration of entering suspension indicated that the value of this parameter was invariant. Comparison of experimental data with predictions obtained using the random walk model showed that the model developed in this paper is more realistic in predicting formation damage. The effect of variations and overlap in the particle size and pore size distributions on the extent of damage to the porous formation have also been described. The model has then been used to predict the minimum cut-off point for prefiltration when straining is the dominant mechanism of particle capture.

NOTATION

A	cross-sectional area of the core
C	concentration of particles in suspension
D_{pa}	mean particle size in the injected suspension
D_{pc}	mean particle size in the filter cake
D_{po}	mean pore size
k_2	constant
$K/K0$	permeability ratio
L	length of the filter cake
$N(D)$	number density
FS	filter cut-off size
p	fraction of bonds in the network
PV	volume of fluid in pore space in network or core
ΔP_c	pressure drop through a filter cake
q	flow rate of the suspension
$R(p)$	percolation probability
s_p	surface area of one particle
UF	unfiltered
v	superficial velocity of the suspension
v_p	volume of one particle

Greek letters

σ_{pa}	particle size standard deviation
σ_{po}	pore size standard deviation
ρ	density of the suspension
ϕ	porosity of the filter cake
μ	viscosity of the suspension

REFERENCES

Donaldson, E. C. and Baker, B. A., 1977, Particle transport in sandstones. SPE 6905.

Dullien, F. A. L. and Dhawan, G. K., 1974, Characterization of pore structure by a combination of quantitative photomicrography and mercury porosimetry. *J. Colloid Interface Sci.* **47**, 337–349.

Fatt, I., 1956, The network model of porous media. *Pet. Trans. AIME* **207**, 144–181.

Fisher, M. E., 1971, The theory of critical point singularities. *Proc. Int. School of Physics*, ENRICO FERMI, pp. 1–99.

Herzig, J. P., LeClerc, D. M. and LeGeoff, P., 1970, Flow of suspensions through porous media—application to deep filtration. *Ind. Engng Chem.* **62**, 8–35.

Jerauld, G. R., Hatfield, J. C., Scriven, L. E. and Davis, H. T., 1984, Percolation and conduction of Voronoi and triangular networks: a case study in topological disorder. *J. Phys. C.* **17**, 3429–3439.

Lapidus, G. R., Lane, A. M., Ng, K. M. and Conner, W. C., 1985, Interpretation of mercury porosimetry data using a pore-throat network model. *Chem. Engng Commun.* **38**, 33–56.

Leichtberg, S., Pfeffer, R. and Weinbaum, S., 1976, Stokes flow past finite coaxial clusters of spheres in a circular cylinder. *Int. J. Multiphase Flow* **3**, 147–169.

Porter, K., 1985, Gulf Oil, Calgary, Alberta (personal communication).

Rose, W., 1957, Studies of waterflood performance—III. Use of network models. *Illinois State Geological Survey Circular* **237**, 1–31.

Sahimi, M., Davis, H. T. and Scriven, L. E., 1983, Dispersion in disordered porous media. *Chem. Engng Commun.* **23**, 329–341.

Siegel, R. A. and Langer, R., 1986, A new Monte Carlo approach to diffusion in constricted porous geometries. *J. Colloid Interface Sci.* **109**, 426–440.

Simon, R. and Kelsey, F. J., June 1971, The use of capillary tube networks in reservoir perfomance studies—I. *Soc. Petrol. Engng J.* 99–112; Part II, August 1972, 345–351.

Tien, C. and Payatakes, A. C., 1979, Advances in deep bed filtration. *A.I.Ch.E. J.* **25**, 737–759.

Todd, A. C., Somerville, J. E. and Scott, G., 1984, The application of depth of formation damage measurements in predicting water injectivity decline. SPE 12498, in press for SPEJ.

Wardlaw, N. C., 1976, Pore geometry of carbonate rocks as revealed by pore cases and capillary pressure. *AAPG Bull.* **60**, 245–257.

Yadav, G. D., Dullien, F. A. L., Chatzis I. and MacDonald, I. F., 1984, Microscopic distribution of wetting and nonwetting phases in sandstones during immiscible displacements. SPE 13212.

Yortsos, Y. C. and Sharma, M. 1986, Application of percolation theory to noncatalytic gas–solid reactions. *A.I.Ch.E. J.* **32**, 46–55.

Zenz, F. A. and Othmer, D. F., 1960, *Fluidization and Fluid-Particle Systems*, pp. 94–135. Reinhold.

APPENDIX

Calculation of filter cake resistance

The pressure drop through a filter cake can be written as

$$-\Delta P_c = [(1-\phi)/\phi^3]\,(s_p/v_p)\{5\mu v(1-\phi)\,(s_p/v_p) + k_2 v^2 \rho\}\,L. \quad \text{(A1)}$$

For laminar flow conditions the second term on the right is

negligible. The length, L, of the filter cake formed on the face of the core can be written as,

$$L = (\text{volume of solids}/A(1-\phi). \quad \text{(A2)}$$

In performing the filter cake pressure drop calculations we shall consider the worst case i.e. assume that all the injected particles formed the cake. The total number of particles injected for a sample run (Run No. 2) during the time interval of 300 min (the time for an entire run) is given by,

$$\text{Number of particles injected} = qC\Delta t$$
$$= 2.78 \times 1.04\text{E}5 \times 300$$
$$= 8.67 \times 10^7 \text{ particles.}$$

To determine the volume of these particles we use the average size of the particles in the cake as 4.6 microns [reported by Donaldson (1977)].

The total volume of solids $= \pi D_{pc}^3 (8.67 \times 10^7)/6 \times 1\text{E} - 6\,\text{m}^3$

$$= 4.42 \times 10^{-9}\ \text{m}^3. \quad \text{(A3)}$$

Other data required in eqs (1) and (2) are shown below. The values for velocity and cross-section area of the core are those used by Donaldson and coworkers in their experiments. The value of (s_p/v_p) is calculated for an average particle size of 4.6 microns.

Given data

$\mu = 1.\text{E} - 3$ kg/m-s $\quad \rho = 1000$ kg/m^3

$v = 1.821\text{E} - 4$ m/s $\quad s_p/v_p = 1.3\text{E} - 2\ \text{m}^{-1}$.

$A = 2.545\text{E} - 4\ \text{m}^2$

Substituting these values and eq. (3) in eqs (1) and (2), and using conversion factors we get,

$$-\Delta P_c = 3.902 \times 10^{-3}[(1-\phi)/\phi^3] \quad \text{in psig.} \quad \text{(A4)}$$

The cubic dependence of $-\Delta P_c$ on ϕ in the denominator indicated that the highest pressure drop would result when ϕ was a minimum. Work done by Zenz and Othmer (1960) shows that the minimum value of ϕ [for the worst case of a closest fitting three component system is 0.12 (Fig. on p. 112 in Reference Zenz and Othmer, 1960)]. Substituting $\phi = 0.12$ we get,

$$-\Delta P_c = 2 \text{ psig}$$

i.e. the worst pressure drop is 2 psig.

In experiments performed by Donaldson, the measured pressure drop was as high as 400–700 psig. Since the worst pressure drop due to filter cake is only 2 psig, the major pressure drop was due to the plugging of the pores in the entry face.